H_2Open Journal

IWA PUBLISHING

H_2Open Journal Vol 4 No 1, 291 doi: 10.2166/h2oj.2021.123

Hen feather: a bio-waste material for adsorptive removal of methyl red dye from aqueous solutions

Samina Zaman*, Md. Nayeem Mehrab, Md. Shahnul Islam, Gopal Chandra Ghosh and Tapos Kumar Chakraborty

Department of Environmental Science and Technology, Jashore University of Science and Technology, Jashore 7408, Bangladesh
*Corresponding author. E-mail: saminazaman25@gmail.com

ABSTRACT

This study investigates the potential applicability of hen feather (HF) to remove methyl red (MR) dye from aqueous solution with the variation of experimental conditions: contact time (1–180 min), pH (4–8), initial dye concentration (5–50 mg/L) and adsorbent dose (3–25 g/L). Scanning electron microscopy (SEM) and Fourier transform infrared spectroscopy (FTIR) evaluate the surface morphology and chemistry of HF, respectively. The maximum removal of MR by HF was 92% when the optimum conditions were initial MR dye concentration 5 mg/L, pH 4, adsorbent dose 7 g/L and 90 min equilibrium contact time. Langmuir isotherm ($R^2 = 0.98$) was more suited than Freundlich isotherm ($R^2 = 0.96$) for experimental data, and the highest monolayer adsorption capacity was 6.02 mg/g. The kinetics adsorption data fitted well to pseudo-second-order model ($R^2 = 0.999$) and more than one process was involved during the adsorption mechanism but film diffusion was the potential rate-controlling step. The findings of the study show that HF is a very effective and low-cost adsorbent for removing MR dye from aqueous solutions.

Key words: adsorption, anionic dye, biosorbent, isotherms, kinetics

HIGHLIGHTS

- An adsorbent was adopted from hen feather (HF) a bio-waste material.
- About 92% methyl red dye removed by HF.
- Equilibrium data followed Langmuir isotherm and the highest monolayer adsorption capacity of HF was 6.02 mg/g.
- Kinetic data followed pseudo-second-order kinetic.

INTRODUCTION

Water is necessary for every survival but nowadays water pollution by discharging different toxic chemicals from the industrial and urban area is a matter of global concern (Shakoor & Nasar 2016). Among the numerous toxic chemicals, dyes in industrial effluents are highly familiar (Subbaiah & Kim 2016). Dyes are commonly used for coloring purpose in different industries such as food, textiles, cosmetics, leather, printing, paper, rubber, plastics and cosmetics (Sharma *et al.* 2011). Discharge from these industries of colored wastewater in water bodies can create inescapable difficulties because it limits the photosynthesis rate by reducing sunlight infiltration rate into the receiving water and gradually makes the unstable condition in aquatic ecosystem (Mubarak *et al.* 2017). Dyes and their degraded byproducts are considered as mutagenic, toxic and carcinogenic nature, so it is comparatively risky for the environment as well as living beings if they are exposed to these substances even at low levels (Huang *et al.* 2017). Dyes may also create severe human health problems such as skin irritation, dermatitis, cancer, abdominal discomfort, damage of liver, kidneys and reproductive system, jaundice and tumors (León *et al.* 2016). Methyl red (MR) is an anionic azo dye used in scientific tests, textile and other business purposes; this causes skin, eye and digestive tract discomfort, pharyngeal or digestive tract irritation if swallowed or inhaled (Muthuraman & Teng 2009) and other health hazards. The removal of MR dye is difficult due to its aromatic ring structure, oxidation reaction and highly light stability (León *et al.* 2016). From an ecological point of view, dyes from polluted water must be removed before being released into the environment, so the selection of applicable and relevant treatment method is most significant for the elimination of dyes from the wastewater. Diverse methods (e.g. adsorption, flocculation, electrolysis, oxidation, ion-exchange, biodegradation, Fenton chemical

oxidation, photocatalysis, etc.) for removing MR dye from wastewater have been applied (Bhatnagar & Sillanpää 2010). Among these methods, adsorption has been considered as most popular in the aspect of cost-effectiveness, operational simplicity and low energy requirements (Ghosh *et al.* 2018). Various types of biomaterials (e.g. natural, agricultural and industrial wastes/byproducts) for dyes removal from wastewater have been investigated, including sawdust, pine leaves, sugarcane bagasse, fly ash, residue sludge, peanut husk, tea waste, orange peel, jute fiber, chitosan, activated carbon (Yagub *et al.* 2014), jute stick (Chakraborty *et al.* 2020) and bark (Ghosh *et al.* 2020). Globally, poultry processing companies create 8.5 billion tons of trash annually (Sarita & Neeraj 2010) and it is a big problem for managing these wastes. The scientific use of feathers as a removable material offers considerable environmental and economic benefits (Gupta *et al.* 2006). Hen feather (HF) exhibits tremendous adsorption capacity for removing several harmful metal ions (Al-Asheh & Banat 2003; Teixeira & Ciminelli 2005) from the wastewater as well as it is available, non-soluble and non-toxic. Therefore, it is a distinct idea to use HF to remove MR from wastewater. The objectives of this research are to examine the effectiveness of HF in aqueous solution for removing MR, by the influencing of different experimental parameters, including contact time, pH, adsorbents dose and initial MR concentration, and finally evaluate the adsorption behavior of HF by adsorption kinetics and adsorption isotherms.

MATERIALS AND METHODS

Adsorbent preparation

HF was collected from a local poultry farm in Jashore, Bangladesh. After collection, it was rinsed with tap water numerous times and then distilled water for dirt removal, dried at 80 °C for 24 h in an oven (Labtech LDO-150F, Korea). After that, the soft barbs were cut into very fine pieces of about 0.1 mm length with the help of scissors and hard stems are discarded, then kept in a hydrogen peroxide (30% w/v) solution for 24 h to remove organic materials. Finally, the adsorbent was rinsed with distilled water and heated for 2 h in the oven at 100 °C. Then, this adsorbent was ready to use and it was stored in airtight borosilicate glass bottles. Table 1 presents the chemical properties of HF.

By the use of a field emission scanning electron microscope (FE-SEM, Zeiss Sigma, Carl Zeiss, Germany), HF surface morphology has been observed (before MR adsorption). FTIR spectra of HF (before adsorption of MR) were recorded by using an FTIR-4600, spectrophotometer (JASCO Corporation Ltd, Japan).

Chemicals and instrumentations

MR dye was purchased from Sigma-Aldrich, USA. Chemical formula $C_{15}H_{15}N_3O_2$; Molecular weight of MR is 269.30 g/mol. Figure 1 shows MR's molecular structure. Analytical grade chemicals were used in this work. The stock solution of MR was made by dissolving the necessary amount of MR powder in double-distilled water. The desired working solution was produced from the stock solution. pH was adjusted by using 0.1M HCl and 0.1M NaOH solution and measured with a digital pH meter (EZdo 6011, Taiwan).

Batch adsorption experiments

Batch testing was carried out using a 250 mL working solution and conducted in 500 mL beaker. In this study, 250 mL known MR solution (made from stock solution dilution) was transferred into individual beaker then pH has been adjusted, a given mass of HF was added to the solution, 200 rpm was set as stirring speed and

Table 1 | Chemical constituents of HF (Mittal *et al.* 2014)

Components	Weight percentage
Crude protein	82
Ash	4
Fat	6
Crude fiber	0.6
Methionine + cysteine	4.9
Lysine	1.8
Metals (Ca, Mg, Se, Zn, etc.)	0.5

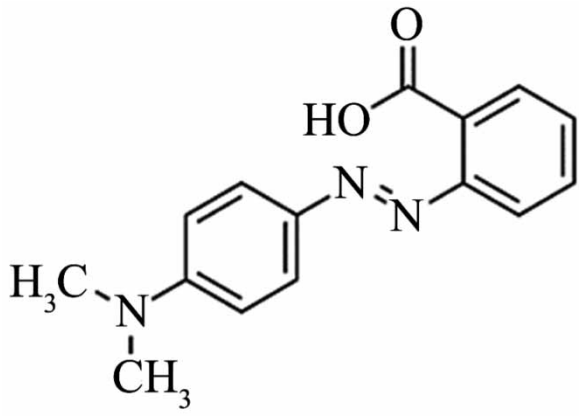

Figure 1 | Molecular structure of MR dye.

temperature of 25 ± 2 °C. The effects of tested conditions: contact time (1–180 min), adsorbent dose (3–25 g/L), pH (4–8) and initial MR concentration (5–50 mg/L) on MR removal by HF were studied by using a Jar-test instrument (JLT4, VELP Scientifics, Italy). After finishing the process, the adsorbent particle sample from the beaker was removed by filtering with the Whatman® glass microfiber filter (GF/B grade).. A UV spectrophotometer (model HACH DR 3900, USA) was used to examine residual MR concentration at 520 nm wavelength. The MR uptake q_e (mg/g) and the MR removal percent R (%) are calculated by using the following equations, respectively.

$$q_e = \frac{(C_0 - C_e)V}{m} \tag{1}$$

$$R\ (\%) = \frac{(C_0 - C_e)}{C_0} \times 100 \tag{2}$$

where C_0 and C_e are the initial and at equilibrium MR concentrations in mg/L, respectively. q_e is the equilibrium MR adsorbed in mg/g. V is the volume of solution (L) and m is the mass of adsorbent (g). Adsorption experiments have been performed in duplicates and the results are averaged.

Isotherm experiments

MR adsorption onto HF was carried out in adsorption isotherm tests with equilibrium contact duration of 90 min in optimum circumstances at pH 4 and stirred with 200 rpm using different initial MR concentration (5–50 mg/L) with 7 g/L fixed HF dose. Langmuir and Freundlich isotherms model were applied in this study. Langmuir isotherm (Langmuir 1918) states monolayer adsorption on fixed site of adsorbent surface, where single adsorbate molecule can take place a single vacant space and no further overlapping at that site. The linear form of the Langmuir isotherm model is presented as

$$\frac{C_e}{q_e} = \frac{1}{q_{max} b} + \frac{C_e}{q_{max}} \tag{3}$$

where q_{max} is the full monolayer coverage quantity of MR (mg/g), and Langmuir constant b (L/mg) is associated with adsorption capacity. When graphing C_e/q_e vs C_e, Langmuir parameters can be calculated. In terms of the dimensionless division factor R_L, the basic properties of the Langmuir equation may be represented as

$$R_L = \frac{1}{1 + bC_0} \tag{4}$$

R_L value indicates the adsorption process, when $R_L > 1$, unfavorable; $R_L = 1$, linear; $0 < R_L < 1$, favorable; and $R_L = 0$, irreversible.

The isotherm model Freundlich is an empirical equation that explains the heterogeneous adsorbent surface and capacity for adsorption depend on adsorbent concentration (Dadfarnia *et al.* 2015). The linearized equation for

the Freundlich isotherm (Freundlich 1906) is expressed in the following equation:

$$\log q_e = \log K_f + \frac{1}{n} \cdot \log C_e \tag{5}$$

where K_f (mg/g) and n are Freundlich constants representing adsorption capacity and intensity, respectively. A linear plot of $\log q_e$ vs $\log C_e$ can calculate K_f and n.

Kinetic experiments

The adsorption kinetics of MR adsorbent was examined by using the pseudo-first-order model, the pseudo-second-order model, the intraparticle diffusion model and the liquid film diffusion model. The linearized form of the kinetic model equation pseudo-first-order is written as follows (Lagergren 1898):

$$\log (q_e - q_t) = \log q_e - \frac{K_1}{2.303} t \tag{6}$$

where q_t is the amount of MR adsorbed (mg/g) at time t and K_1 is the pseudo-first-order rate constant. The plot of $\log(q_e - q_t)$ vs t should provide a linear connection. The slope and the intercept of the plot can determine K_1 and q_e, respectively.

The pseudo-second-order equation can be represented as a linear form in Equation (7) (Ho & McKay 1999)

$$\frac{t}{q_t} = \frac{1}{K_2 q_e^2} + \frac{1}{q_e} t \tag{7}$$

The constant K_2 is used to calculate the initial adsorption rate (h), at $t = 0$, as follows:

$$h = K_2 q_e^2 \tag{8}$$

The linear plot of t/q_t vs t shows $1/q_e$ as the slope and $1/K_2 q_e^2$ as the intercept and the parameter can be calculated from here.

The intraparticle diffusion model was discovered by Weber and Morris equation (Weber & Morris 1963). This model shows the presence of the intraparticle diffusion through the adsorption procedure. Equation (9) represented the intraparticle diffusion model.

$$q_t = K_{id} t^{0.5} + C \tag{9}$$

where K_{id} is the constant rate of intraparticle diffusion (mg/g.min$^{0.5}$) calculable in the linear plot slope q_t against $t^{0.5}$. C is the plot intercept that indicates the effect of the boundary layer. Greater surface adsorption contribution to the rate control step when the intercept is higher (Wu *et al.* 2005).

Liquid film diffusion model is applied to study adsorption kinetics and mechanisms of MR removal by HF. These models are expressed as

$$\ln(1 - F) = -K_{fd} t \tag{10}$$

where F is the equilibrium fractional attainment ($F = q_t/q_e$), K_{fd} is the constant of liquid film diffusion. A linear plot from $\ln(1 - F)$ vs t with zero intercepts would recommend that the sorption process kinetics was influenced by diffusion.

RESULTS AND DISCUSSION

Adsorbent characterization

The FTIR analysis was utilized to detect adsorbent surface chemistry. Figure 2 shows the FTIR of HF. The adsorption peak at 2,875.86 cm^{-1} (C–H stretching vibration) and 3,606.89 cm^{-1} (O–H stretching vibration of hydroxyl group) was the primal peak of HF. The C = O stretching vibration of ketones, carboxylic anhydrides and lactones was found at 1,739.79 and 1,627.92 cm^{-1}. The amide II of the peak was at 1,521.84 cm^{-1}. The other peaks at

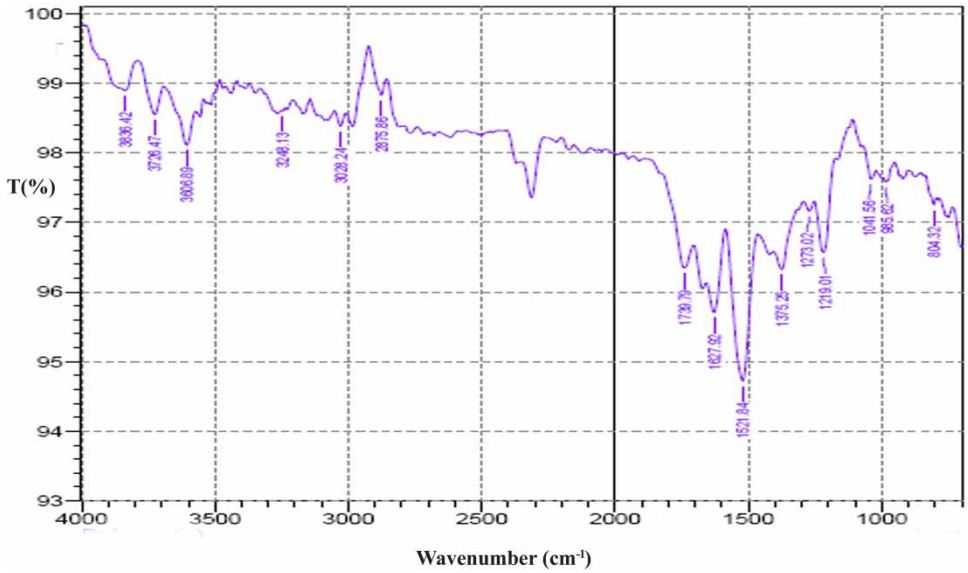

Figure 2 | FTIR spectra of HF (before adsorption of MR).

1,041.56 cm^{-1} (C–C skeleton vibration); 985.62 cm^{-1} (C–H out-of-plane deformation vibration) and 804.32 cm^{-1} (C–O–C stretching vibration, $=CH_2$ twisting vibration) was observed in HF.

Scanning electron microscopy (SEM) has been utilized to characterization the surface morphology of adsorbents. The feather's side branches are called barbs and are joined by a group of barbs. Barbs have their own side branches named barbules. The SEM image of HF is shown in Figure 3. The surface of HF showed uneven, irregular spaces of various shapes and sizes which can be used for adsorption of MR. Sun *et al.* (2009) have noticed a similar finding.

Effect of contact time and pH

The experiment was conducted at equilibrium condition: initial 20 mg/L MR dye concentration, HF dose (7 g/L), pH (4) and temperature of (25 $\pm$ 2 °C) to evaluate the effect of contact time for removal of MR, as presented in Figure 4(a). MR dye removal efficiency and adsorption capacity by HF increased when the adsorption time increased and rise dramatically in the initial 20 min, and after that time it increased slowly and equilibrium reached at 90 min (Figure 4(a)). A higher adsorption rate was found at the primary stage due to the availability of vacant sites on the adsorbent source. Additionally, MR dye removal and adsorption rates were decreased due to the occupied of HF external adsorption sites by MR dye molecules with time progress. However, no significant

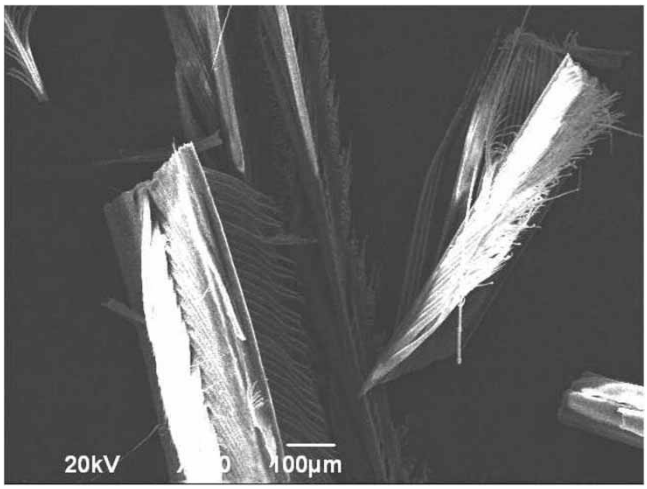

Figure 3 | SEM image of HF (before adsorption of MR).

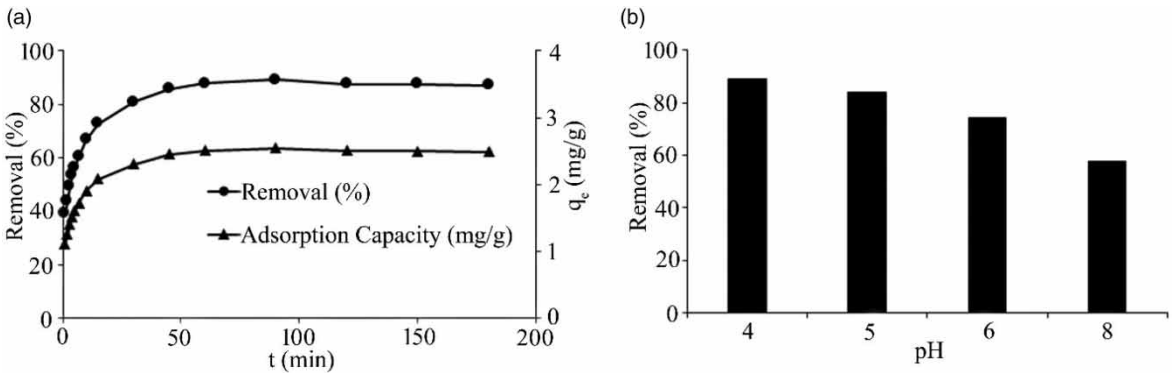

Figure 4 | Effect of (a) contact time and (b) pH on removal of MR by HF (where rotation speed (200 rpm), adsorbent dose (7 g/L), temperature (25 ± 2 °C) and initial MR dye concentration (20 mg/L)).

change was observed after 90 min. So, further batch experiments were conducted at 90 min equilibrium contact time.

On the other hand, experiments were carried out at the initial MR concentration of 20 mg/L, 7 g/L HF dose, starring speed of 200 rpm, at 25 ± 2 °C temperature and 90 min equilibrium contact time with different pH ranges (4–8) in order to determine the effects of pH on MR adsorption by HF, as presented in Figure 4(b). The efficacy of MR removal dropped by 89 to 57% with increasing studied pH (4–8) (Figure 4(b)). pH not only affects the adsorbent's surface load but also the degree of color ionization in solution during the adsorption process. A maximum MR dye removal (89%) was found at pH 4 (Figure 4(b)), because at acidic pH, the adsorbent surface is positively charged due to protonation, which increased the electrostatic attraction between adsorbent and adsorbate, this might be leads to the maximum MR removal (Saad *et al.* 2007). Conversely, the removal efficiency decreased at higher pH due to the increase of competition for adsorption sites between excess OH^- ions and anionic MR dye molecules.

Effect of adsorbent dose and initial MR concentration

The adsorption of MR onto HF was examined by the variation of HF dose (3–25 g/L) in solution while keeping the other operation parameters constant; equilibrium contact time of 90 min, initial MR dye concentration of 20 mg/L, starring speed of 200 rpm, pH 4 and temperature of 25 ± 2 °C. The removal of MR increased from 87 to 92% when the HF dose increased from 3 to 25 g/L, due to the increasing surface area and more binding adsorption sites. On the other hand, the adsorption rate was gradually reduced (5.80–0.74 mg/g) with the same dose shown in Figure 5(a). On the other hand, the adsorption capacity was decreased with increase HF dose because of the particle interaction, for example aggregation, resulting from reduced the total adsorbent surface area (Aksakal & Ucun 2010). Ghosh *et al.* (2020) found a similar trend for removing anionic dye from aqueous solution by biosorbent.

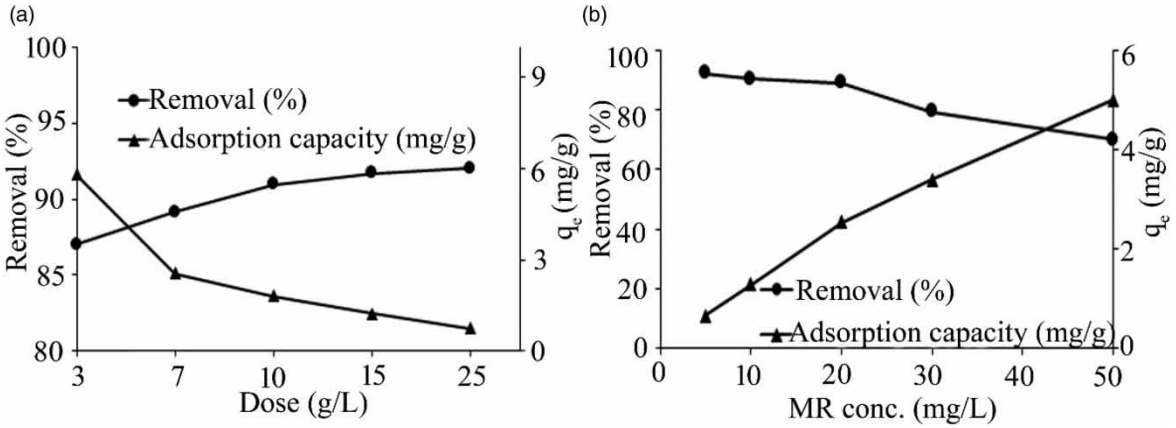

Figure 5 | Effect of (a) adsorbent dose and (b) initial MR concentration on removal of MR by HF (where rotation speed (200 rpm), pH (4), contact time (90 min) and temperature (25 ± 2 °C)).

Adsorption experiments with the variation of initial MR dye concentrations (5–50 mg/L) were carried out at a fixed HF dose of 7 g/L, pH of 4, starring speed of 200 rpm, temperature of 25 ± 2 °C for 90 min equilibrium contact time. The findings indicated that the HF adsorption capacity increased (0.66–5.01 mg/g) with increasing initial MR concentration (5–50 mg/L) due to the mass transfer resistance of the dye between the solid and aqueous phases, which improved the interaction of MR molecules and HF surface. On the other hand, the removal of MR gradually reduced from 92 to 70% shown in Figure 5(b), because at the constant dose, the adsorbent external surface is saturated as well as dye molecules block the pores of the adsorbent (Chowdhury & Saha 2010). So, the removal efficiency significantly depends on the initial MR concentration and contact time.

Adsorption isotherms

The adsorption isotherm is significant for describing the common behavior among the adsorbent and the solutes, and it is also important for the adsorption system design (Dadfarnia *et al.* 2015). In this study, the isothermal models of Langmuir and Freundlich were used to explore the MR adsorption behaviors onto HF. The linearized form of the isotherm and calculated parameters are presented in Figure 6 and Table 2, respectively. On the basis of correlation coefficient (R^2) value, the Langmuir isotherm model ($R^2 = 0.98$) fitted better as compared with the Freundlich model ($R^2 = 0.96$), indicating that MR molecules create monolayer coverage with homogenous nature onto HF surface and the maximum adsorption capacity was 6.02 mg/g (Table 2). The separation factor (R_L) value (0.41–0.065) was less than 1 but greater than 0, suggesting that the MR adsorption onto HF is suitable. Moreover, the Freundlich constant value ($n = 1.83$) was greater than 1 and higher K_f value (1.288) indicating a favorable behavior toward MR adsorption.

HF absorption capacity is compared with other adsorbents, as presented in Table 3. From the table, it shows that HF is a suitable and alternative adsorbent for the removal of MR from aqueous solution, for its low cost and easy availability.

Adsorption kinetics

In this study, four kinetic models (Lagergren pseudo-first-order, Ho's pseudo-second-order, intraparticle diffusion and liquid film) were applied to determine the adsorption behavior of MR onto HF, as presented in Figure 7, and the model's parameters values are given in Table 4. The higher R^2 and calculated ($q_{e,cal}$) value was found for the pseudo-second-order kinetic model than the pseudo-first-order kinetic model (Table 4), confirming that the

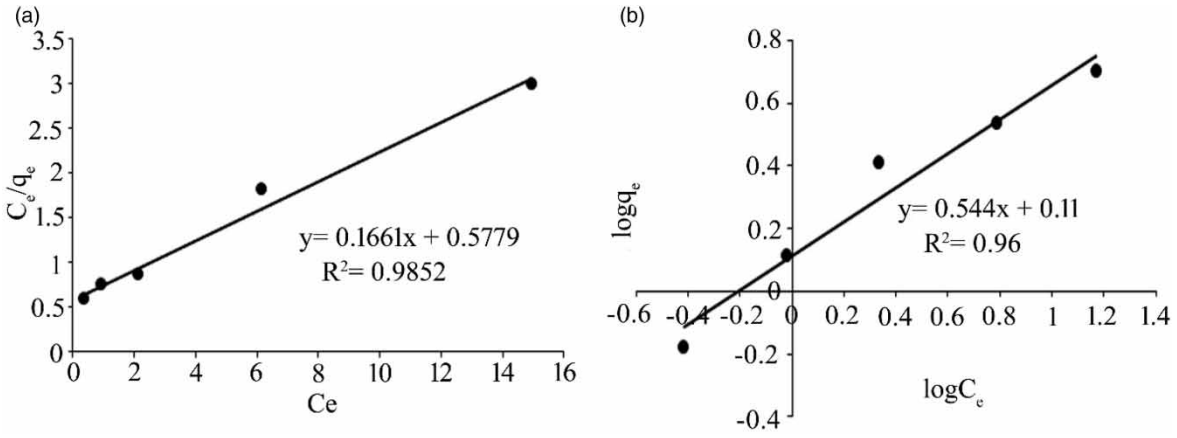

Figure 6 | Adsorption isotherm plot of MR onto HF using different isotherm models: (a) Langmuir isotherm and (b) Freundlich isotherm.

Table 2 | Isotherm parameters for MR adsorption onto HF

Langmuir isotherm				Freundlich isotherm		
q_{max} (mg/g)	b (L/mg)	R^2	R_L	K_f (mg/g)	N	R^2
6.02	0.287	0.98	0.41–0.065	1.116	1.838	0.96

Table 3 | Comparison of MR dye adsorption capacity by HF with other adsorbents

Adsorbents	Maximum adsorption capacity (mg/g)	Optimum dose (g/L)	Concentration range (mg/L)	References
Annona squmosa Seed (CAS)-activated carbon	40.486	4	25–200	Santhi *et al.* (2010)
Thiosemicarbazide-modified chitosan	17.31	3.33	10–60	Mozaffari *et al.* (2019)
Phosphoric acid-treated sugarcane bagasse	10.98	4	50–250	Saad *et al.* (2010)
Modified zeolite	7	24	200	Ioannou *et al.* (2013)
Hen feather	6.02	7	5–50	This study
Sugarcane bagasse	5.66	4	50–250	Saad *et al.* (2010)
Spent oil shale	3.8	0.6	10–100	Mahmoud *et al.* (2020)

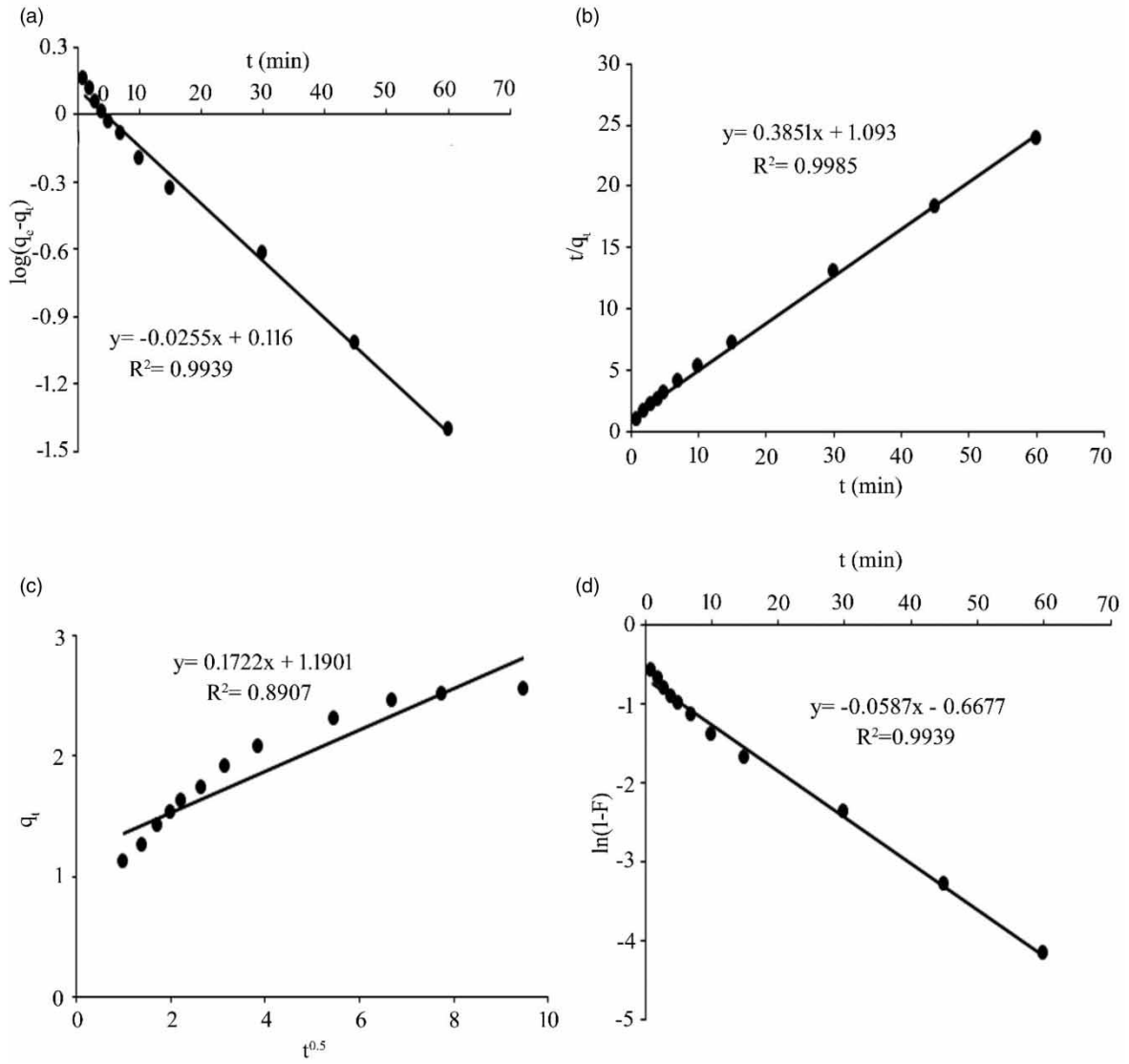

Figure 7 | Adsorption kinetic of MR onto HF using different kinetic models: (a) pseudo-first-order, (b) pseudo-second-order, (c) intraparticle diffusion and (d) liquid film.

Table 4 | Kinetic parameters for MR adsorption onto HF

Models	Parameters	Values
Pseudo-first-order	$q_{e,exp}$ (mg/g)	2.547
	q_e (mg/g)	1.123
	K_1	−0.059
	R^2	0.994
Pseudo-second-order	q_e (mg/g)	2.597
	K_2	0.136
	R^2	0.999
	h (mg/g/min)	0.915
Intraparticle diffusion	K_{id} (mg/g.min$^{0.5}$)	0.172
	C	1.19
	R^2	0.891
Liquid film	K_{fd}	0.059
	R^2	0.994

adsorption process follows the pseudo-second-order kinetic model. So, the whole adsorption processes seem to be controlled by chemisorption, i.e. the electrostatic interactions between the surface of the positively charged HF and negatively charged MR molecules. The experimental data were further analyzed by intraparticle diffusion in order to investigate the diffusion mechanisms. The intraparticle diffusion plot did not pass through the origin (Figure 7(c)) and higher intercept value ($C = 1.19$) (Table 3), indicating that multi-diffusion was involved during MR adsorption onto HF such as external diffusion (i.e. agglomerate of MR molecules on the adsorbent surface) and internal diffusion (i.e. transport of MR molecules inside the adsorbent particle), that may occur simultaneously. Moreover, the liquid film plot showed that film diffusion was the rate-limiting step for adsorption of MR onto HF because the plot was linear and did not pass through the origin (Figure 7(d)).

CONCLUSION

The usability of HF to remove MR dye from aqueous solution was investigated under different experimental conditions, such as pH, contact time, initial MR dye concentration and adsorbent dosage. A maximum MR dye removal was detected at pH 4. The HF efficiency for MR dye removal was 92%, from solutions containing 5 mg/L of dye at adsorbent dose of 7 g/L. The Langmuir isotherm fit better with the experimental data as well as the maximum adsorption capacity was 6.02 mg/g. Kinetic studies show that the adsorption process followed the pseudo-second-order kinetic model with multi-steps diffusion process, and film diffusion was the potential rate-limiting step. The study of the FTIR and SEM showed that the HF surface has distinct function groups and more porous active sites for MR dye adsorption. Finally, it concluded that, for the removal of MR from aqueous solutions, HF is an available, effective and low cost/no cost adsorbent.

ACKNOWLEDGEMENTS

We would like to thank the Department of Environmental Science and Technology, Jashore University of Science and Technology, Bangladesh, for providing the necessary support. We also thank the Ministry of Science and Technology, Bangladesh, for the research grant (R&D) award.

CONFLICT OF INTEREST

The authors declare that they have no competing interests.

FUNDING

The authors would like to thank the Ministry of Science and Technology, Bangladesh, for the research grant (R&D) award.

DATA AVAILABILITY STATEMENT

All relevant data are included in the paper or its Supplementary Information.

REFERENCES

Aksakal, O. & Ucun, H. 2010 Equilibrium, kinetic and thermodynamic studies of the biosorption of textile dye (Reactive Red 195) onto *Pinus sylvestris* L. *Journal of Hazardous Materials* **181** (1–3), 666–672. https://doi.org/10.1016/j.jhazmat.2010.05.064.

Al-Asheh, S. & Banat, F. 2003 Beneficial reuse of chicken feathers in removal of heavy metals from wastewater. *Journal of Cleaner Production* **11** (3), 321–326. https://doi.org/10.1016/S0959-6526(02)00045-8.

Bhatnagar, A. & Sillanpää, M. 2010 Utilization of agro-industrial and municipal waste materials as potential adsorbents for water treatment – a review. *Chemical Engineering Journal* **157** (2–3), 277–296. https://doi.org/10.1016/j.cej.2010.01.007.

Chakraborty, T. K., Islam, M. S., Zaman, S., Kabir, A. H. M. E. & Ghosh, G. C. 2020 Jute (*Corchorus olitorius*) stick charcoal as a low-cost adsorbent for the removal of methylene blue dye from aqueous solution. *SN Applied Sciences* **2** (4), 1–10. https://doi.org/10.1007/s42452-020-2565-y.

Chowdhury, S. & Saha, P. 2010 Sea shell powder as a new adsorbent to remove Basic Green 4 (Malachite Green) from aqueous solutions: equilibrium, kinetic and thermodynamic studies. *Chemical Engineering Journal* **164** (1), 168–177. https://doi.org/10.1016/j.cej.2010.08.050.

Dadfarnia, S., Shabani, A. H., Moradi, S. E. & Emami, S. 2015 Methyl red removal from water by iron based metal-organic frameworks loaded onto iron oxide nanoparticle adsorbent. *Applied Surface Science* **330**, 85–93. https://doi.org/10.1016/j.apsusc.2014.12.196.

Freundlich, H. M. F. 1906 Over the adsorption in solution. *Journal of Physical Chemistry* **57** (385471), 1100–1107.

Ghosh, G. C., Samina, Z. & Chakraborty, T. K. 2018 Adsorptive removal of Cr (VI) from aqueous solution using rice husk and rice husk ash. *Desalination and Water Treatment* **130**, 151–160. https://doi.org/10.5004/dwt.2018.22828.

Ghosh, G. C., Chakraborty, T. K., Zaman, S., Nahar, M. N. & Kabir, A. H. M. E. 2020 Removal of methyl orange dye from aqueous solution by a low-cost activated carbon prepared from mahagoni (*Swietenia mahagoni*) bark. *Pollution* **6** (1), 171–184. doi:10.22059/poll.2019.289061.679.

Gupta, V. K., Mittal, A., Kurup, L. & Mittal, J. 2006 Adsorption of a hazardous dye, erythrosine, over hen feathers. *Journal of Colloid and Interface Science* **304** (1), 52–57. https://doi.org/10.1016/j.jcis.2006.08.032.

Ho, Y. S. & McKay, G. 1999 Pseudo-second order model for sorption processes. *Process Biochemistry* **34** (5), 451–465. https://doi.org/10.1016/S0032-9592(98)00112-5.

Huang, R., Liu, Q., Huo, J. & Yang, B. 2017 Adsorption of methyl orange onto protonated cross-linked chitosan. *Arabian Journal of Chemistry* **10** (1), 24–32. https://doi.org/10.1016/j.arabjc.2013.05.017.

Ioannou, Z., Karasavvidis, C., Dimirkou, A. & Antoniadis, V. 2013 Adsorption of methylene blue and methyl red dyes from aqueous solutions onto modified zeolites. *Water Science and Technology* **67** (5), 1129–1136. https://doi.org/10.2166/wst.2013.672.

Lagergren, S. 1898 Zur theorie der sogenannten adsorption geloster stoffe. *Kungliga Svenska Vetenskapsakademiens Handlingar* **24** (4), 1–39.

Langmuir, I. 1918 The adsorption of gases on plane surfaces of glass, mica and platinum. *Journal of the American Chemical Society* **40** (9), 1361–1403. https://doi.org/10.1021/ja02242a004.

León, G., García, F., Miguel, B. & Bayo, J. 2016 Equilibrium, kinetic and thermodynamic studies of methyl orange removal by adsorption onto granular activated carbon. *Desalination and Water Treatment* **57** (36), 17104–17117. https://doi.org/10.1080/19443994.2015.1072063.

Mahmoud, N. A., Nassef, E. & Husain, M. 2020 Use of spent oil shale to remove methyl red dye from aqueous solutions. *AIMS Materials Science* **7** (3), 338–353. doi:10.3934/matersci.2020.3.338.

Mittal, A., Thakur, V., Mittal, J. & Vardhan, H. 2014 Process development for the removal of hazardous anionic azo dye Congo red from wastewater by using hen feather as potential adsorbent. *Desalination and Water Treatment* **52** (1–3), 227–237. https://doi.org/10.1080/19443994.2013.785030.

Mozaffari, M., Emami, M. R. S. & Binaeian, E. 2019 A novel thiosemicarbazide modified chitosan (TSFCS) for efficiency removal of Pb (II) and methyl red from aqueous solution. *International Journal of Biological Macromolecules* **123**, 457–467. https://doi.org/10.1016/j.ijbiomac.2018.11.106.

Mubarak, N. S. A., Jawad, A. H. & Nawawi, W. I. 2017 Equilibrium, kinetic and thermodynamic studies of Reactive Red 120 dye adsorption by chitosan beads from aqueous solution. *Energy, Ecology and Environment* **2** (1), 85–93. doi:10.1007/s40974-016-0027-6.

Muthuraman, G. & Teng, T. T. 2009 Extraction of methyl red from industrial wastewater using xylene as an extractant. *Progress in Natural Science* **19** (10), 1215–1220. https://doi.org/10.1016/j.pnsc.2009.04.002.

Saad, R., Belkacemi, K. & Hamoudi, S. 2007 Adsorption of phosphate and nitrate anions on ammonium-functionalized MCM-48: effects of experimental conditions. *Journal of Colloid and Interface Science* **311** (2), 375–381. https://doi.org/10.1016/j.jcis.2007.03.025.

Saad, S. A., Isa, K. M. & Bahari, R. 2010 Chemically modified sugarcane bagasse as a potentially low-cost biosorbent for dye removal. *Desalination* **264** (1–2), 123–128. https://doi.org/10.1016/j.desal.2010.07.015.

Santhi, T., Manonmani, S. & Smitha, T. 2010 Removal of methyl red from aqueous solution by activated carbon prepared from the *Annona squmosa* seed by adsorption. *Chemical Engineering Research Bulletin* **14** (1), 11–18. https://doi.org/10.3329/cerb.v14i1.3767.

Sarita, A. & Neeraj, W. 2010 Degradation of chicken feather a poultry waste product by Keratinolytic bacteria isolated from dumping site at Ghazipur poultry processing plant. *International Journal of Poultry Science* **9** (5), 482–489.

Shakoor, S. & Nasar, A. 2016 Removal of methylene blue dye from artificially contaminated water using citrus limetta peel waste as a very low cost adsorbent. *Journal of the Taiwan Institute of Chemical Engineers* **66**, 154–163. https://doi.org/10.1016/j.jtice.2016.06.009.

Sharma, P., Kaur, H., Sharma, M. & Sahore, V. 2011 A review on applicability of naturally available adsorbents for the removal of hazardous dyes from aqueous waste. *Environmental Monitoring and Assessment* **183** (1), 151–195. https://doi.org/10.1007/s10661-011-1914-0.

Subbaiah, M. V. & Kim, D. S. 2016 Adsorption of methyl orange from aqueous solution by aminated pumpkin seed powder: kinetics, isotherms, and thermodynamic studies. *Ecotoxicology and Environmental Safety* **128**, 109–117. https://doi.org/10.1016/j.ecoenv.2016.02.016.

Sun, P., Liu, Z. T. & Liu, Z. W. 2009 Particles from bird feather: a novel application of an ionic liquid and waste resource. *Journal of Hazardous Materials* **170** (2–3), 786–790. https://doi.org/10.1016/j.jhazmat.2009.05.034.

Teixeira, M. C. & Ciminelli, V. S. 2005 Development of a biosorbent for arsenite: structural modeling based on X-ray spectroscopy. *Environmental Science and Technology* **39** (3), 895–900. https://doi.org/10.1021/es049513m.

Weber Jr., W. J. & Morris, J. C. 1963 Kinetics of adsorption on carbon from solution. *Journal of the Sanitary Engineering Division* **89** (2), 31–59. https://doi.org/10.1061/JSEDAI.0000430.

Wu, R., Qu, J. & Chen, Y. 2005 Magnetic powder MnO–Fe_2O_3 composite – a novel material for the removal of azo-dye from water. *Water Research* **39** (4), 630–638. https://doi.org/10.1016/j.watres.2004.11.005.

Yagub, M. T., Sen, T. K., Afroze, S. & Ang, H. M. 2014 Dye and its removal from aqueous solution by adsorption: a review. *Advances in Colloid and Interface Science* **209**, 172–184. https://doi.org/10.1016/j.cis.2014.04.002.

First received 16 August 2021; accepted in revised form 1 October 2021. Available online 14 October 2021